

Accuracy of three-dimensional measurement using a single image

Pio Iovenitti, MEMBER SPIE
Swinburne University of Technology
Industrial Research Institute Swinburne
John Street
Hawthorn 3122, Australia
E-mail: piovenitti@swin.edu.au

Abstract. The accuracy of 3-D measurement using a single image of a four-point coplanar target of known size is studied. The factors that influence accuracy are analyzed and experimental techniques are used to establish their individual effect on accuracy. Experiments show that the four-point coplanar target has two solutions for real images and that mixing these causes large errors. It is concluded that when the target is approximately parallel to the image plane, the accuracy is significantly better compared to other target orientations, and that image distance is a critical factor affecting accuracy in the depth, while the effect of the other factors on accuracy is relatively insignificant. A new calibration technique is introduced that determines an average image distance over the image plane within the depth of focus and improves accuracy at close range.
© 1997 Society of Photo-Optical Instrumentation Engineers.

Subject terms: three-dimensional measurement; image analysis; perspective four-point problem.

Paper 10076 received July 11, 1996; accepted for publication Sep. 6, 1996.

1 Introduction

Accurate measurement of a 3-D position using computer vision is achieved by those methods based on triangulation. These methods use either multiple images from different viewpoints, such as in photogrammetry,¹ or a single image and a fixed sheet of light combined with known movement of the object to be measured.² A single image provides accurate measurement in the two dimensions parallel to the image plane, but poor accuracy in the depth. Many techniques for determining position using a single 2-D image have been proposed, and all depend on known geometric patterns or objects. The most widely used geometry for single-image techniques has been the three or more point featured shapes of either the coplanar or noncoplanar type.³⁻¹⁰ These geometric targets have been used to calibrate camera parameters as well as to determine the orientation and position of objects.

Extracting orientation and position from a single image has applications in robotics, for grasping objects, and in navigation of autonomous vehicles. Success in these applications depends on algorithms that can reliably produce unique solutions with minimal processing time. The range of measurement in such cases can vary from 0.5 to 5 m, and the accepted uncertainty of measurement can be several centimeters. To extend the application of single image techniques to other areas of industry, such as digitizing a component's surface geometry as input to a CAD system, requires precision.

The accuracy of measurement for methods using a single image of a target is subject to various limitations:

1. uncertainty inherent in the method and its algorithm
2. uncertainty associated with the sensor and image digitization
3. uncertainty of the optical parameters
4. variability of environment conditions.

The effects of these factors on the accuracy of 3-D coordinate measurement using a single image of a known target have not been quantified in the past. This paper presents the results of a study, which is analytical and experimental, of the effects of the salient factors on the accuracy of 3-D measurement using a single image. Also, the included survey of other similar methods highlights the accuracy that has been achieved so far in this area.

2 Method for Determining 3-D Coordinates

The method for determining the 3-D coordinates of a point in front of a camera involves the use of a square target with 50-mm sides.¹¹ The square is defined by 1-mm-thick white lines on a black background. From Fig. 1, the six dimensions defining the target, TB , TR , TL , RL , RB , and BL , are accurately measured and used to calculate the target's position from its perspective image. A set of trigonometric equations relate the vertices of the target to their corresponding image coordinates in the camera coordinate system. Geometric information about an object can be found by means of vertex T , which is in contact with the object. To find the coordinates of the target's four vertices, the image distance, pixel size, and image center must be known, and the coordinates of the vertices in the image plane must be found by image analysis. The latter is achieved by scanning the image, and as a target line is detected, its centroid is calculated. A least-squares method is used to fit lines of best fit to the centroids, and the four vertices of the image are found by the intersections of the four lines. It is essential to use the centroid of the lines and not the edge to determine the vertices because the

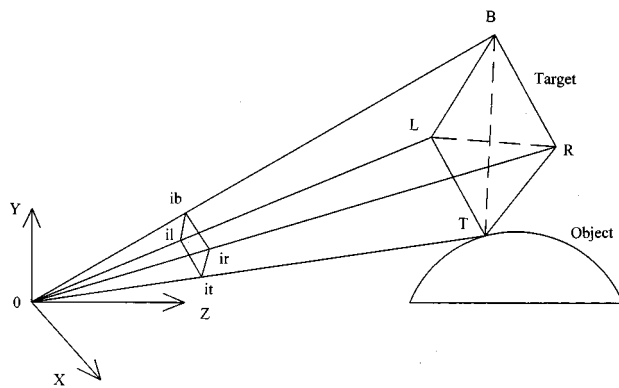


Fig. 1 Camera coordinate system, image plane, and the target representation. The image plane is parallel to the xy plane, and the z axis lies along the optical axis of the lens. The optical center of the lens is the origin.

linewidths change with threshold, aperture setting, and lighting conditions, whereas the centerlines of the lines remain unaffected.

A solution is found by an iteration process that is begun by choosing an initial value for the distance from the optical center to point T , OT . From this initial choice the other three vertices are found. After the first iteration, the size of the target is determined. The algorithm is such that three of the six dimensions (TR , RB , and BL) will be equal to the measured values, and the other three (TL , TB , and RL) will differ from the measured values. The sum of the absolute differences between the latter three dimensions and their true size is found. Successive increments in OT are dependent on the magnitude of the sum of differences, and the algorithm finds the minimum sum of differences. The distance corresponding to this minimum difference is taken as the solution. For the experiments reported in Table 10, the average minimum sum of differences was 0.147 mm, with a standard deviation of 0.066 mm.

This method is appropriate for this study because it is robust. The algorithm always converges to a solution and it is not sensitive to small variations in parameter values or lighting conditions.

The camera used in this study was a Pulnix TM-765E with a CCD sensor having 756 horizontal (H) \times 581 vertical (V) pixels, with 256 gray levels. The pixel size, according to the manufacturer's specification, is $11 \times 11 \mu\text{m}$. Two lenses were used, one a Cosmimar/Pentax $f/1.4$, 25-mm TV lens, the other a Xenoplan 1:1.9/25 low-distortion lens from Schneider Optische Werke Kreuznach GMBH & Co. The Xenoplan lens uses a compound lens system with a stop in between the lenses. The frame grabber was an Oculus MX set up to produce an image size of 768 (H) \times 574 (V).

3 Effect of Method on Accuracy

3.1 Algorithm for Determining 3-D Coordinates

A four-point coplanar target was used to minimize the number of possible solutions for a given image when determining position. The four-point problem should have a unique solution,^{4,12,13} but experiments revealed that there were two possible solutions to the four-point coplanar problem for real images. In the range 700 to 900 mm, the dif-

Table 1 Typical results showing two solutions for vertex T using a real image.

Nominal Distance (mm)	Solution Number	Calculated Position for Vertex T (mm)		
		x	y	z
760	1	-43.02	21.21	766.71
	2	-43.65	21.51	777.75
Difference		0.63	0.30	11.04
860	1	33.17	-41.21	879.17
	2	33.59	-41.73	890.38
Difference		0.42	0.52	11.21

ference between the two solutions for the T_z coordinate was 11 to 14 mm, while the difference for T_x and T_y was less than 1 mm, see Table 1. The existence of two solutions can be explained by the fact that real perspective images are imperfect, and that an algorithm will find the nearest solution(s). Mixing these solutions caused large errors when determining the distance between two points, whereas using the same solution produced good results.

3.2 Positioning and Support of Target

Since the target is to be positioned on an object to record its shape in terms of point data, the effect of positioning and supporting the target was investigated. The target was positioned and supported by hand on a fixed point, approximately 760 mm from the camera, and its image was recorded. Then, the target was removed and repositioned. Again, the image was recorded. This procedure was repeated until 10 images had been obtained, and a further 10 images were recorded for a point at 880 mm.

This experiment was repeated with the target positioned by hand but supported by a stand to avoid movement and blurred images. The results in Table 2 show that supporting the target by hand caused greater variations in T_x and T_z compared to a target supported by a stand. The variation in T_y was smallest in both cases because the contact point restricts movement in this direction.

3.3 Target Orientation

The effect of target orientation on the accuracy of measurement was investigated. The target was supported by a stand on a fixed point, approximately 750 mm from the camera, and maintaining the target in a vertical position, 10 images were recorded with the target at various angles to the image plane. The results in Table 3 show that T_z was significantly affected, with a standard deviation of 3.05 mm, due to two

Table 2 Effect of method of support on vertex T .

Target Support Method	Hand		Stand	
Distance of target (mm)	760	880	760	880
Vertex T (std. dev.)				
x (mm)	0.30	0.49	0.15	0.09
y (mm)	0.05	0.06	0.04	0.01
z (mm)	1.33	1.22	0.67	0.79

Table 3 Effect of the target orientation on calculated position.

Vertex T (mm)	Standard Deviation
x	0.24
y	0.09
z	3.05

clusters of solutions approximately 6 mm apart. The value of T_x was slightly affected, with a standard deviation of 0.24 mm, which may have been partly due to positioning, and T_y was unaffected. When the target orientation was approximately parallel to the image plane, the variation in calculated position was negligible. This target orientation was used for all other experiments reported in this paper.

4 Effect of Optical Parameters on Accuracy

4.1 Image Distance

The image distance was analyzed for its effect on the accuracy of measurement because it is one of the major parameters that determines the target position in the depth.

The relationship between focal length and image distance for a thin lens is given by

$$\frac{1}{ID_f} = \frac{1}{f} - \frac{1}{OD_f}, \quad (1)$$

where

ID_f = focused image distance

f = focal length

OD_f = object distance.

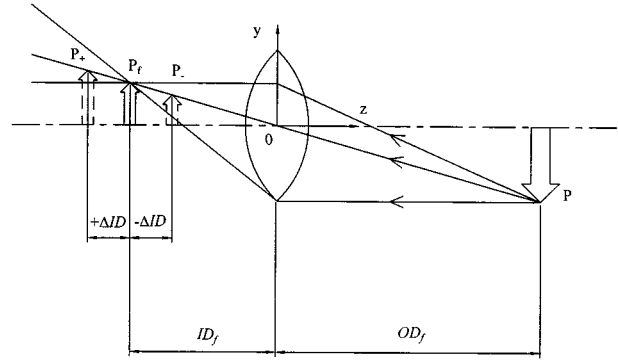
For applications of computer vision where the object distance is several meters, the focal length is used to determine position, since image distance approaches the focal length for large object distances. If the object distance is small, say 0.5 to 1 m, and the object distance changes, then the focused image distance varies significantly, hence for accurate determination of position, the image distance must be known precisely.

It is shown that a 0.1-mm discrepancy in image distance from the true value can cause an error of 3 mm in position for an object distance of 800 mm. Referring to Fig. 2, if the sensor is moved away from the lens and focused image position ID_f the image height changes. Assuming that the center of the target lies on the optical axis and the target is parallel to the image plane, as shown in Fig. 3, let OD_f be the focused object distance and ID_f the corresponding focused image distance. If the sensor is moved by an amount ΔID away from the lens, there is an increase in the height of the image of Δr , and the image appears larger. The relation between Δr and ΔID is given by

$$\frac{\Delta r}{\Delta ID} = \frac{r_f}{ID_f} = \tan(\theta) = \frac{R}{OD_f}, \quad (2)$$

where R is half the diagonal length of the target and r_f is the height of the focused image.

From Eq. (1),


Fig. 2 Effect on the image height of a point P by movement of the sensor from the focused position.

$$ID_f = \frac{OD_f f}{OD_f - f}, \quad (3)$$

$$r_f = \frac{RID_f}{OD_f}. \quad (4)$$

If ID_f is used to determine the object distance, then

$$OD = \frac{RID_f}{r_f + \Delta r}, \quad (5)$$

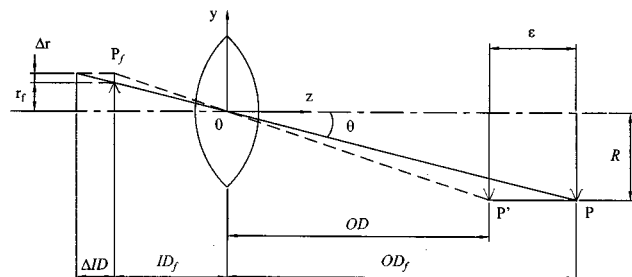
and the error in object distance ϵ is

$$\epsilon = OD_f - OD. \quad (6)$$

For example, if $OD_f = 800$ mm, $f = 25$ mm, and $\Delta ID = 0.1$ mm, the calculated object distance equals 796.91 mm, and the error in object distance is -3.09 mm. The target appears closer to the lens. Similarly, a 0.1-mm displacement of the sensor toward the lens, will cause an error of $+3.11$ mm; the target appears smaller and farther from the lens.

Equation (6) is further developed to include ΔID . Substituting for ID_f , r_f , and Δr using Eqs. (2), (3), and (4), the calculated object distance, given by Eq. (5), becomes

$$OD = \frac{OD_f^2 f}{OD_f(f + \Delta ID) - \Delta ID f}. \quad (7)$$


Fig. 3 Effect on the calculated object distance by an error of ΔID .

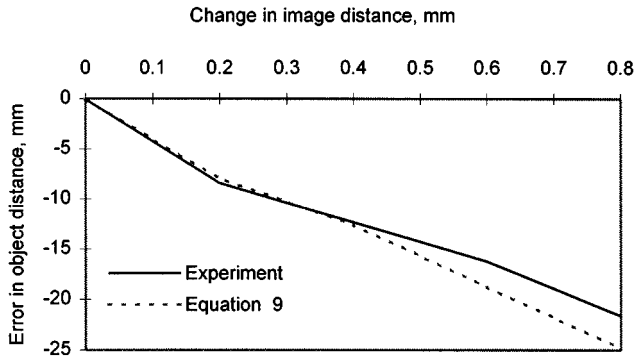


Fig. 4 Effect of increasing image distance, by adjusting focus, on the error in calculated object distance for a target at 800 mm.

Since ΔID_f is small, an approximate expression for OD is

$$OD = \frac{OD_f f}{f + \Delta ID} \quad (8)$$

and the error in object distance defined by Eq. (6), is now given by

$$\epsilon = OD_f \left(\frac{f}{f + \Delta ID} - 1 \right) \quad (9)$$

Equation (9) shows that as the object distance increases, the error in the calculated object distance also increases due to a discrepancy of ΔID in the image distance. Conversely, as the object distance reduces, the error also reduces for the same ΔID .

Experiments were carried out to verify Eq. (9). Using the Cosmocar lens with a focal length of 25 mm, the lens was focused on the target, fixed at a distance of 800 mm, and its image recorded. Then, the focus was altered so that the image distance increased, and a second image recorded. The focus was adjusted several more times and further images were recorded. Target distance Tz was then determined for each image using the same ID value [calculated from Eq. (1)]. The differences in calculated distance caused by changing the focus were found and compared to the results from Eq. (9). Changing the focus caused a displacement of the lens relative to the target, however, the effect of this on the object distance was negligible and ignored. Figure 4 shows that there is good agreement between Eq. (9) and experimental results, and demonstrates the effect of image distance on the calculated position. The experimental results also show that there is a linear relationship between ΔID and ϵ with a correlation coefficient of 0.998 and an error of -2.28 mm per 0.1-mm change in ID. Further experiments at 800 mm using the Cosmocar and Xenoplan lenses gave results of -2.99 and -3.15 mm per 0.1-mm increase in ID.

4.2 Calibration for Image Distance within the Depth of Focus

The accuracy of 3-D measurement within the depth of focus is dependent on a precise knowledge of the image distance. Finding the image distance involved positioning the

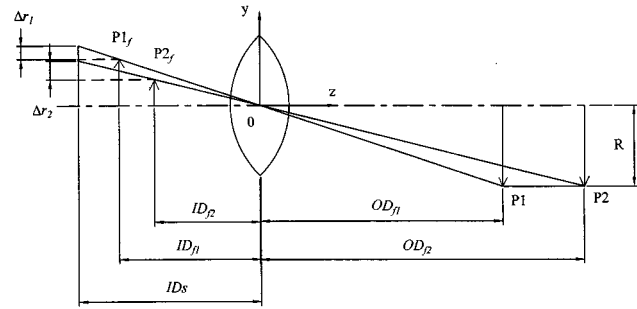


Fig. 5 Calibration model for IDs using two points.

target at two points, at approximately 680 and 780 mm, and recording their images. The distance between these two points, in the direction of the optical axis, was accurately measured to be 100 mm. The Cosmocar lens was focused on a point at 760 mm.

Using the two images, the distance between the two points was calculated for various values of ID. The difference between the true distance and the calculated distances ϵ_{12} for each ID value is shown later in Fig. 6. For ID equal to 26.2 mm the error was zero. This value of ID is subsequently referred to as the set ID, ID_s . At an object distance of 760 mm, the focused image distance is 25.85 mm for a thin lens using Eq. (1). In this case, the ID_s value is higher than the value determined using the thin lens equation.

This experiment was repeated many times with different arrangements and with the Xenoplan lens. In each case, provided that the target was approximately parallel to the image plane an ID_s was found that eliminated error within the depth of focus. An analytic model for this calibration technique is developed later that relates the relative error ϵ_{12} , the OD, and the ID_s to an arbitrarily chosen ID referred to as ID_c .

If the ID_s is unknown, what is the effect of wrongly choosing a value for ID to determine distances within a range of OD_1 and OD_2 ? Referring to Fig. 5, the calculated positions of the target at points 1 and 2 are given by

$$OD_{c1} = \frac{RID_c}{r_1} \quad (10a)$$

$$OD_{c2} = \frac{RID_c}{r_2} \quad (10b)$$

Assuming that $ID_s > ID_{f1}$ and $ID_s > ID_{f2}$, where ID_{f1} and ID_{f2} are the focused IDs for points 1 and 2, and ID_s and ID_c are as already defined. The image heights are given by

$$r_1 = r_{f1} + \Delta r_1 \quad (11a)$$

$$r_2 = r_{f2} + \Delta r_2 \quad (11b)$$

where

$$r_1 \text{ and } r_2 = \text{heights of out-of-focus image points 1 and 2}$$

r_{f1} and r_{f2} = heights of the image for focused points 1 and 2
 Δr_1 and Δr_2 = displacements of image points 1 and 2 caused by out of focus.

Expressions for Δr_1 and Δr_2 , determined from Fig. 5, are

$$\Delta r_1 = \frac{\Delta ID_{f1} R}{OD_{f1}}, \tag{12a}$$

$$\Delta r_2 = \frac{\Delta ID_{f2} R}{OD_{f2}}. \tag{12b}$$

The differences between the IDs's and the focused image distances for points 1 and 2 are

$$\Delta ID_{f1} = ID_s - ID_{f1}, \tag{13a}$$

$$\Delta ID_{f2} = ID_s - ID_{f2}. \tag{13b}$$

The errors in object distance for points 1 and 2 are

$$\epsilon_1 = OD_{c1} - OD_{f1}, \tag{14a}$$

$$\epsilon_2 = OD_{c2} - OD_{f2}. \tag{14b}$$

Using Eqs. (4), (10), (12), and (13), the expressions for ϵ_1 and ϵ_2 become

$$\epsilon_1 = OD_{f1} \left(\frac{ID_c}{ID_s} - 1 \right), \tag{15a}$$

$$\epsilon_2 = OD_{f2} \left(\frac{ID_c}{ID_s} - 1 \right). \tag{15b}$$

If the distance between points 1 and 2 is considered, the relative error is

$$\epsilon_{12} = \epsilon_2 - \epsilon_1, \tag{16}$$

and substituting Eq. (15) gives

$$\epsilon_{12} = (OD_{f2} - OD_{f1}) \left(\frac{ID_c}{ID_s} - 1 \right). \tag{17}$$

From Eq. (17), when ID_c is equal to ID_s the error in the distance between points 1 and 2 is zero. The ID_s value, found by experiment, was used in Eq. (17) and the error in relative distance was calculated for various values of ID_c . The results in Fig. 6 show good agreement between the experimental results and Eq. (17).

Further calibration experiments were conducted to determine ID_s for nine locations in the image plane. The results in Fig. 7 show that the average value of ID_s was 27.062 mm with a standard deviation of 0.1222 mm. This variation suggests that the sensor (image plane) is not parallel to the plane of lens. Other calibration methods produce a single value for image distance.

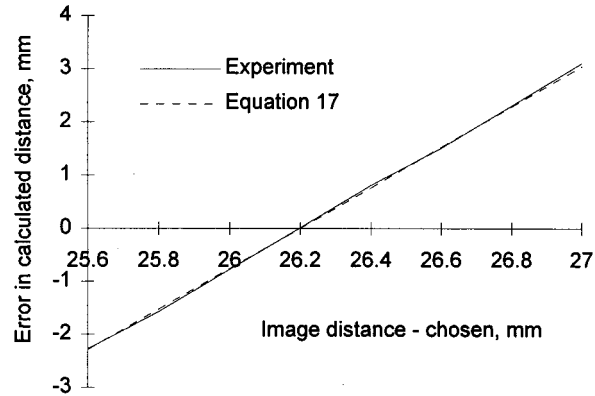


Fig. 6 Variation of error in relative distance measurement ϵ_{12} with ID_c .

4.3 Lens Distortion

A compound lens with a stop in between can provide images that are relatively free of distortion.¹⁴ Using a low-distortion lens, such as the Xenoplan lens, can reduce the effect of distortion. Past research shows that the image distortion for this type of lens is of the order of 0.1 pixel, whereas a Cosmimar lens may give distortions of up to 0.7 pixels.¹⁵

4.4 Aperture Setting

The aperture setting, or f -number, controls the amount of light passing through the lens. It also controls the depth of focus, which is the distance an object may move in the z direction and still maintain a sharp image.¹⁶ To increase the depth of focus the aperture size should be reduced, for example, changing from $f/2$ to $f/5.6$. The effect of varying the aperture is linear so that depth of focus at $f/16$ is 8 times that of $f/2$.

A low f -number enables light through the lens periphery, which has poor manufacturing quality, with the result being barrel or pincushion distortion. For a high f -number, the opening may no longer be circular, and light falling on the sensor can be modulated across its surface, thus affect-

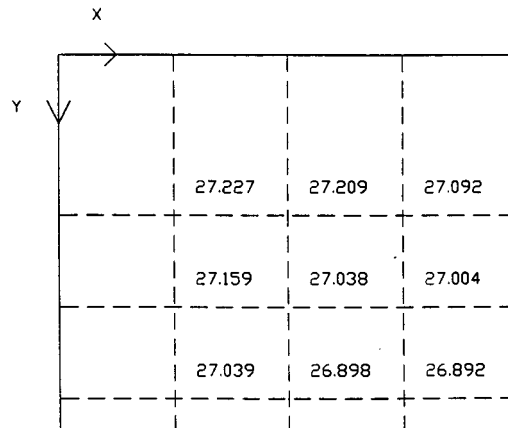


Fig. 7 Variation of IDs in the image plane using a Xenoplan lens.

Table 4 The effect of aperture setting on the image and vertex T using an Xenoplan lens with a range of $f/1.9$ to $f/16$.

Aperture Setting, f -number	11	8	5.6
Background, gray level	0–10	0–10	0–15
Target, gray level	10–80	10–135	15–255
Line width, average, pixels	2.64	3.72	5.42
Vertex T (std. dev.)			
x (mm)		0.01	
y (mm)		0.01	
z (mm)		0.08	

ing contrast. A high f -number setting approximates a pin-hole camera, which has no distortion.¹⁴ Thus, for low distortion and a high depth of focus, an intermediate setting would be required. Experiments were carried out to determine the effect of aperture setting on the calculated target position.

The target was placed at a distance of approximately 800 mm, and images were recorded for various aperture settings of the Xenoplan lens. The variation in gray levels, target linewidths, and calculated target position for each case is shown in Table 4. The background and target gray levels and the line widths were significantly affected, while the centerlines of the target were unaffected. Since the algorithm detects and uses the centerlines to calculate position, position was also unaffected, as shown by the low standard deviation. An intermediate aperture setting of $f/5.6$ was used for all other experiments with the Xenoplan lens.

5 Effect of Sensor and Image Digitization on Accuracy

5.1 Pixel Width and Height

The effect of pixel width and pixel height is to displace the calculated target position along the z axis in the camera coordinate system. For relative measurement, small variations in pixel size are not significant, however, for absolute measurement, accurate parameter values are necessary.¹¹

A good estimate of the pixel width can be obtained by multiplying width by the ratio of camera sampling frequency (14.1875 Mhz) to the frame grabber sampling rate (14.75 Mhz); in this case, 0.01058 mm. A slightly higher value, 0.0107 mm/pixel, was used because it performed better in experiments. The manufacturer's vertical pixel height specification can be used without calibration for a solid state camera. In this case the pixel height is 0.011 mm.

5.2 Threshold

The effect of varying the threshold on the image coordinates and vertex T of the target is shown in Table 5. The image coordinates for the target vertices and the vertex T were calculated using threshold gray level values between 60 and 140 for two target distances, 700 and 800 mm. The effect on the calculated position was negligible. At 800 mm, the standard deviation for T_z was 0.13 mm. Increasing the threshold from 60 to 140 reduced the line width de-

Table 5 The effect of threshold value on the image coordinates and calculated target position.

Threshold range, gray level	60 to 140	
Target distance (mm)	700	800
Image vertices (std. dev.)		
x, y coordinates (pixels)	0.04	0.08
Vertex T (std. dev.)		
x (mm)	0.01	0.02
y (mm)	0.01	0.01
z (mm)	0.07	0.13

tected (from 6 to 4 pixel width at 700 mm, and from 4 to 2.5 pixel width at 800 mm), but did not change the image coordinates for the vertices.

5.3 Image Center

If the image center is offset from its true position, the calculated target position in the xy plane of the camera coordinate system is also offset. From the various calibration methods for image center that are available,¹⁷ the varying focal length technique was adapted by using a fixed target position and focus adjustment. The graphical solution to locate the image center was similar to the one used with Moffitt's principal point locator,¹⁸ although the apparatus and technique differed. The calibrated image centers for the camera lens systems are reported in Table 6 as offsets referred to the frame buffer center.

5.4 Image Digitization

An experiment was conducted to assess the effect of the image digitization process on accuracy.^{19,20} The target was positioned at 600 mm and 10 images were recorded in succession, and their positions determined. This was repeated for a target distance of 700 mm. After calculating the standard deviations for the three coordinates of T , the results in Table 7 show that image digitization has a negligible effect on T_x and T_y , and that T_z is only slightly sensitive, with a standard deviation of 0.06 mm.

6 Effect of Environment Conditions on Accuracy

6.1 Lighting

Three combinations of lighting were used to determine the effect of lighting conditions on the calculated position. A fluorescent desk lamp and fluorescent room lighting provided light sources that would commonly be available. Three combinations of lighting were used in the experiments: lamp and room lighting, lamp only, and room lighting only. Lighting had little effect on the calculated target

Table 6 Image centers for the Pulnix camera with the lenses used in the experiments.

Image Center	Cosmicar Lens	Xenoplan Lens
x offset (pixels)	38.5	29.55
y offset (pixels)	-23.0	39.47

Table 7 Effect of image digitization on target position.

Distance of Target (mm)	600	700
Vertex T (std. dev.)		
x (mm)	0.02	0.02
y (mm)	0.01	0.01
z	0.03	0.06

position, as shown in Table 8, even though the detected target line thickness changed from approximately 7 pixels (lamp and room lighting) to 3 pixels (room lighting only).

6.2 Temperature

The effect of temperature change on the performance of the camera was also investigated by taking measurements during the warm-up stage of the camera. The target was supported on a single point, which was located approximately 680 mm from the camera. The camera was switched on and images were recorded at intervals of 5 to 45 min. Table 9 shows that the results for a cold camera are similar to that of a warm camera.

7 Measurements Using the Target

To assess the overall accuracy of measurement the coordinates of five points, located between 700 and 800 mm from the camera, were measured using the target, which was positioned by hand and supported by a stand. Distances between these points were also measured using a standard measuring instrument for comparison.

Ten sets of readings were taken for each point using the target, and the calculated coordinates of the five points are shown in Table 10. The errors of measurement are shown in Table 11. The average error in distance was 1.32 mm with a standard deviation of 0.9 mm. An average value of 26.92 mm for IDs was determined by calibrating the camera with the Xenoplan lens.

In practice, points are usually measured to find the distances between them or to find information about a geometric feature on an object. Coordinate measurement machines (CMM) are normally used to measure points belonging to a particular geometric feature of an object and fit mathematical surfaces, such as a plane or sphere, to them.

To assess the accuracy in measuring geometric features twelve points on a planar surface (130×110 mm), located at a distance of 750 mm, were measured using the target, and a least-squares plane of best fit and its flatness were calculated. Considering the extreme point on each side of the fitted plane, flatness is defined as the distance between these two points in a direction normal to the plane. This

Table 8 The effect of various lighting levels on calculated target position at a distance of 700 mm.

Vertex T (mm)	Standard Deviation
x	0.04
y	0.03
z	0.13

Table 9 Effect of camera temperature on vertex T .

Vertex T (mm)	Standard Deviation
x	0.04
y	0.02
z	0.05

was repeated for two other orientations of the surface. The three orientations are illustrated in Fig. 8. The results in Table 12 show that when the plane was approximately normal to the image plane, the accuracy was very good and compared with the CMM measurement, whereas other orientations showed relatively large flatness values.

8 Survey of Other Methods Using Single Images

A review of other methods also using single images to determine 3-D position from known geometry constraints was carried out to find what accuracy has been achieved. In most instances, the accuracy achieved by the method was reported and is also presented here, in others, no information related to accuracy was reported.

A comprehensive survey of range imaging techniques is provided by Besl.²¹ The nominal accuracy achieved by the scene constraint methods (computer vision), which included the known geometry methods, are of the order of 1 mm and the maximum nominal depth of field is 100 m. He concludes that the metrology potential of these techniques has not been demonstrated, they are computationally intensive, and have a limited capability, but offer an inexpensive solution to range measurement.

Triangular pairs were used by Linnainmaa et al.⁵ to estimate the location and pose of a 3-D object of known size, however, the accuracy of their method in determining location was not reported.

Fukui⁹ used a square pattern, 230-mm sides with 20-mm-wide edges, to determine radial distance using single images. Movement of his target was constrained in one plane, the floor, and the radial distances were calculated in this plane. His experiments were carried out in the range of 2 to 5 m. At 2 m, the average error was 9.8 mm.

Hung et al.¹⁰ used a planar quadrangle, of known size and location, within a world reference frame, to determine the position and pose of the camera relative to the fixed world coordinate system. Their simulations were carried out for a range of about 5 m, and their results showed that

Table 10 Calculated coordinates of the five points.

Point	Coordinates (mm)		
	x	y	z
T_1	31.62	25.07	702.91
T_2	56.76	-2.76	777.56
T_3	-31.54	-1.68	811.24
T_4	-62.94	50.21	732.60
T_5	-2.31	49.29	754.40

Table 11 Accuracy of measurement using target.

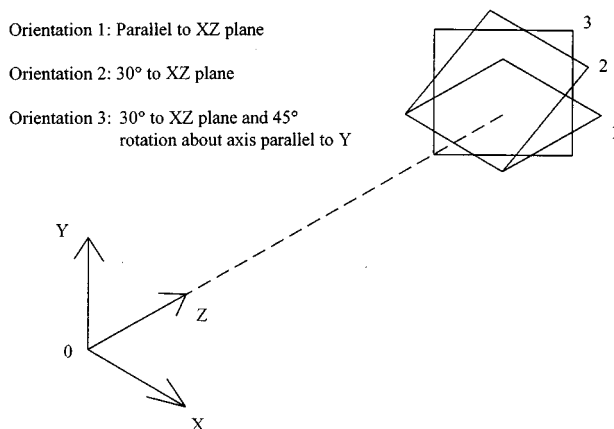
Distance	True Distance (mm)	Error in Measurement Using Target (mm)	
		Maximum	Minimum
$T_1 T_2$	81.2	3.13	1.73
$T_1 T_3$	130.1	1.30	0.13
$T_1 T_4$	102.4	-0.80	0.54
$T_1 T_5$	67.9	-2.00	-0.78
$T_2 T_3$	99.5	-0.63	0.48
$T_2 T_4$	136.3	2.43	1.80
$T_2 T_5$	80.8	1.51	1.01
$T_3 T_4$	95.8	3.15	1.01
$T_3 T_5$	82.1	2.26	0.97
$T_4 T_5$	64.5	-0.43	0.36

the mean error in distance varied from 2 to 75.7 mm using 0.5 and 1.0-pixel perturbations with various sizes of quadrangles.

Haralick⁷ presents a technique using a single perspective image of a rectangle to determine the camera parameters relative to the rectangle. According to Haralick, if the size of the rectangle is known, then the exact coordinates can be computed. No simulation or experimental results were reported.

Yuan⁴ carried out simulations using a target composed of four coplanar feature points at object distances of 1 to 5 m. At 1 m, the positional errors were between 1.43 to 1.95% of the actual distance (14.3 to 19.5 mm) for a 25-mm effective focal length and various orientations of the target.

Raju and Rudraraju⁶ used a single view of four noncoplanar points, whose locations in space were known, to determine the transformation parameters between the camera coordinate system and the base coordinate system. These transformation parameters were then used to determine position from the images of sets of points in other locations. Their experimental results, assuming the unit was

**Fig. 8** Three orientations of plane to evaluate accuracy.**Table 12** Measurement of flatness for three orientations of a plane surface using the target compared to a CMM.

Method	Orientation of Plane		
	Parallel to xz Plane	30 deg to xz Plane	30 deg to xz Plane and 45 deg Rotation
CMM, flatness (mm)	0.0713	0.0713	0.0713
Target, flatness (mm)	0.1311	1.5528	1.8379

inches, gave average errors of 3.56 mm in x , 34.29 mm in y , and 23.43 mm in z within the base coordinate system.

Chen et al.⁸ used cubes of known size (50, 100, 150, and 200 mm) to determine 3-D location and orientation relative to the camera. Their experimental results for the mean positional difference magnitudes for cube location change were 2.0 to 2.5 mm at a distance of 500 mm, using a 50-mm cube, and 5.8 to 48.2 mm at a distance of 1642 mm, using a 200-mm cube. Their results show that the effect of out of focus on the mean positional difference magnitude for the cube location change was 10.94 mm at a distance of 1032.7 mm for a cube size of 100 mm.

Wang and Tsai²² used a 50-mm cube to calibrate the camera parameters that were subsequently used for vehicle guidance. Their experimental results, conducted for vehicle distances ranging from 421 to 1658 mm, showed average errors ranging from 1.9 to 3.0% of the actual distance.

Simulations by Pehkonen et al.³ using a polyhedral object of known dimensions produced average errors of 0.30 mm in the x and y directions and 0.93 in the z direction for the optimized case. Maximum errors were 3.09 mm in the x and y directions and 7.55 mm in the z direction. The range for measurement was -250 to $+250$ in x and y and -250 to -1000 mm in z .

9 Conclusion

Using a single-perspective image of a coplanar four-point target for measurement can provide good accuracy within a plane parallel to the image plane, whereas measurements in the depth are subject to a greater sensitivity. Experiments show that the dominant factors affecting the accuracy of measurement in the depth at close range are method of measurement, target orientation, and image distance. The proposed method minimizes the effect of these factors on accuracy and demonstrates that the accuracy of measurement in the depth can be improved to a level acceptable for applications in industrial design.

References

1. M. R. Shortis and C. S. Fraser, "Dimensional inspection in manufacturing via vision metrology," *Int. Conf. on Manufacturing Engineering*, pp. 415-423 (1995).
2. K. C. Ng and B. F. Alexander, "A high speed noncontact shape measurement system," in *Australasian Instrumentation & Measurement Conf.*, pp. 309-314 (1992).
3. K. Pehkonen, D. Harwood, and L. S. Davis, "Parallel calculation of 3-D pose of a known object in a single view," *Pattern Recog. Lett.* **12**, 353-361 (1991).
4. J. S.-C. Yuan, "A general photogrammetric method for determining object position and orientation," *IEEE Trans. Robot. Automat.* **5**(2), 129-142 (1989).
5. S. Linnainmaa, D. Harwood, and L. S. Davis, "Pose determination of

- a three-dimensional object using triangle pairs," *IEEE Trans. Pattern Anal. Mach. Intell.* **10**(5), 634–647 (1988).
6. G. V. S. Raju and P. Rudraraju, "Camera calibration using distance invariance principles," in *Optics, Illumination, and Image Sensing for Machine Vision V, Proc. SPIE* **1385**, 50–56 (1990).
 7. R. M. Haralick, "Determining camera parameters from the perspective projection of a rectangle," *Pattern Recog.* **22**(3), 225–230 (1989).
 8. Z. Chen, D.-C. Tseng, and J.-Y. Lin, "A simple vision algorithm for 3-D position determination using a single calibration object," *Pattern Recog.* **22**(2), 173–187 (1989).
 9. I. Fukui, "TV image processing to determine the position of a robot vehicle," *Pattern Recog.* **14**(1–6), 101–109 (1981).
 10. Y. Hung, P.-S. Yeh, and D. Harwood, "Passive ranging to known planar point sets," in *Proc. IEEE Int. Conf. on Robotics and Automation*, pp. 80–85 (1985).
 11. P. Iovenitti, W. Thompson, and M. Singh, "Three-dimensional measurement using a single image," *Opt. Eng.* **35**(5), 1496–1502 (1996).
 12. R. Horaud, B. Conio, and O. Le Boulleux, "An analytic solution for the perspective 4-point problem," *Comput. Vis. Graph. Image Process.* **47**, 33–44 (1989).
 13. M. A. Fischler and R. C. Bolles, "Random sample consensus: a paradigm for model fitting with applications to image analysis and automated cartography," *Commun. Assoc. Comput. Mach.* **24**(6), 381–395 (1981).
 14. F. A. Jenkins and H. E. White, *Fundamentals of Optics*, Chap. 9, pp. 171–174, McGraw-Hill, New York (1976).
 15. S. B. Boey, "High accuracy three-dimensional model generation," pp. 58–60, PhD Thesis, Monash Univ., Melbourne (1990).
 16. R. K. Hopwood, "Design considerations for a solid-state image sensing system," in *Minicomputers and Microprocessors in Optical Systems, Proc. SPIE* **230**, 72–82 (1980).
 17. R. K. Lenz and R. Y. Tsai, "Techniques for calibration of the scale factor and image center for high accuracy 3-D machine vision metrology," *IEEE Trans. Pattern Anal. Mach. Intell.* **10**(5), 713–720 (1988).
 18. C. C. Slama, Ed., "Non topographic photogrammetry," in *Manual of Photogrammetry*, Chap. 16, pp. 850–852, American Society of Photogrammetry, Virginia (1980).
 19. U. Ricklefs, "Measurement accuracy of non contact video inspection systems," in *Industrial Inspection II, Proc. SPIE* **1265**, 157–164 (1990).
 20. P. Cencik, "Subpixel edge location shift," *Proc. SPIE* **1822**, 121–131 (1992).
 21. P. J. Besl, "Range imaging sensors," Research Publication GMR-6090, pp. 87–91, General Motors Research Labs., Warren, MI (1988).
 22. L.-L. Wang and W.-H. Tsai, "Computing camera parameters using vanishing-line information from a rectangular parallelepiped," *Mach. Vis. Appl.* **3**, 129–141 (1990).



Pio Iovenitti graduated from the Royal Melbourne Institute of Technology in 1974 and received his MEngSc degree in 1985 from Monash University, Melbourne, Australia. He has been a lecturer with the School of Mechanical and Manufacturing Engineering, Swinburne University of Technology, since 1987, and is a member of the Industrial Research Institute Swinburne, where his current research activities are measurement using machine vision and cutting-tool optimization.